

LA-UR- 93-4450

Title: NIGHTTIME SENSITIVITY OF IONOSPHERIC TECHNIQUES FOR DETECTING EXPLOSIONS

Author(s): T. Joseph Fitzgerald, NIS-1

Submitted to: Department of Energy Headquarters

DO NOT CIRCULATE

PERMANENT RETENTION



Los Alamos NATIONAL LABORATORY



Los Alamos National Laboratory, an affirmative action/equal opportunity employer, is operated by the University of California for the U.S. Department of Energy under contract W-7405-ENG-36. By acceptance of this article, the publisher recognizes that the U.S. Government retains a nonexclusive, royalty-free license to publish or reproduce the published form of this contribution, or to allow others to do so, for U.S. Government purposes. The Los Alamos National Laboratory requests that the publisher identify this article as work performed under the auspices of the U.S. Department of Energy.

# Nighttime Sensitivity of Ionospheric Techniques for Detecting Explosions.

T. Joseph Fitzgerald

*Los Alamos National Laboratory, Los Alamos, New Mexico 87545*

December 14, 1993



## Contents

<b>Abstract</b>	<b>3</b>
<b>1 Introduction</b>	<b>4</b>
<b>2 Ionospheric Detection of Explosions</b>	<b>5</b>
2.1 <i>Nighttime Ionosphere</i> . . . . .	5
2.2 <i>Measurement Technique</i> . . . . .	6
2.3 <i>Hunters Trophy</i> . . . . .	7
<b>3 Non-Proliferation Experiment</b>	<b>9</b>
3.1 <i>Experiment</i> . . . . .	13
3.2 <i>Tonopah Results</i> . . . . .	13
3.3 <i>Los Alamos Results</i> . . . . .	18
<b>4 Discussion</b>	<b>20</b>
4.1 <i>Propagation</i> . . . . .	20
4.2 <i>Prediction of Effects</i> . . . . .	21
4.3 <i>Mining Explosions</i> . . . . .	24
<b>5 Conclusion</b>	<b>26</b>
<b>6 Acknowledgement</b>	<b>27</b>
<b>7 References</b>	<b>27</b>

## Abstract

The detection of explosions using ionospheric techniques relies on measuring perturbations induced in radio propagation by acoustic waves which disturb the electron density of the ionosphere. We have proposed such techniques as a supplement to seismic for discrimination of underground nuclear explosions from commercial mining explosions. The nighttime ionosphere presents a difficulty for the detection of explosions because in the absence of solar ionizing radiation the electron density in the altitude range of 90 to 200 km decays after sunset and perturbation effects are correspondingly reduced. On the other hand, acoustic waves produced by weak explosions reach a maximum amplitude in the altitude range of 100 to 150 km and are highly attenuated at altitudes above 200 km. For safety reasons, most planned explosions are conducted during daylight which has limited our experimental measurements during nighttime. However a recent opportunity for a nighttime measurement occurred in connection with the Non-Proliferation Experiment which consisted of the detonation of a large chemical charge underground at the Nevada Test Site near midnight local time. Our results, based on a new technique of using medium frequency radio transmissions provided by commercial broadcasts to detect explosion effects, were negative. Although discouraging, this result need not defeat our goal of developing an ionospheric technique for discrimination of mining explosions because the majority of such events are conducted during daylight.

## 1 Introduction

The current research project, Explosion Discrimination using Ionospheric Techniques (EDIT), is directed toward developing techniques to discriminate between underground nuclear explosions and commercial mining explosions based on the idea that there would be an ionospheric signature accompanying a mining explosion which would not be present for an underground nuclear explosion. The current project builds on previous research conducted by Los Alamos National Laboratory to detect the signature produced by acoustic waves generated by surface ground motion above an underground nuclear explosion and to relate the magnitude of the ionospheric signature to the yield of the explosion. The major research issues of the first year of the EDIT project concerned the extent of ionospheric perturbations produced by mining explosions. We conducted a series of ionospheric measurements in conjunction with mining explosions and have successfully detected an ionospheric signature for four of these events [Fitzgerald, 1993]. The mechanism that produces an ionospheric signature relies on propagation of airblast from the explosion to the ionosphere.

Our technique detects perturbations imposed on radio waves propagating through the ionosphere by changes in electron density which alter the index of refraction of the radio waves. The electron density changes result from changes in neutral density accompanying acoustic waves which propagate to the ionosphere from the explosion. Thus the detection process demands that the ambient electron density be sufficient that the changes produce a noticeable variation of the index of refraction. The amplitude of acoustic waves from weak sources near ground level reaches a maximum in the altitude range from 100 to 150 km. This maximum occurs because of the competing processes of amplification due to propagation into an increasingly rarefied atmosphere versus attenuation caused by geometric spreading and viscosity. Viscosity increases greatly in the altitude regime for which the neutral mean free path reaches values of the order of the acoustic wavelength which usually occurs above 100 km. The nighttime ionosphere presents a difficulty because the electron density in the lower ionosphere where the acoustic waves reach maximum amplitude decays after sunset. During the daytime the electron density of the lower ionosphere is maintained by two competing processes: production via solar ionizing radiation and recombination via a number of chemical reactions. During the nighttime, the electron density of the lower ionosphere decays by as much as an order of magnitude. On the other hand, diurnal changes in the electron density of the upper ionosphere are less severe because at the lower neutral density the production and recombination mechanisms differ and serve to sustain ionization through the night.

In this report we discuss the problem of explosion detection during nighttime using ionospheric techniques. We present our measurements of two explosions conducted at the Nevada Test Site (NTS). The first was made in conjunction with the Hunters Trophy nuclear test which was conducted during daylight. We employed the technique of reflection of high frequency radio waves to remotely detect acoustic waves produced by ground motion. The second measurement was made in conjunction with the Non-Proliferation Experiment (NPE), the detonation of a 1.4 kt charge of chemical explosive in almost the same location as the Hunters Trophy test. For the NPE measurement, we monitored the ionospheric

reflection of transmissions of medium frequency broadcast stations.

## 2 Ionospheric Detection of Explosions

We have detected the airblast from unconfined explosions with yields of less than one ton using the sensitive technique of observing perturbations induced by acoustic waves on radio signals reflected from the lower ionosphere [Fitzgerald and Carlos, 1992]. This technique, which has been applied by many researchers to detect acoustic waves produced by surface explosions, earthquakes, and underground explosions, relies on the sensitivity of the reflection process to small perturbations in the ionosphere near the reversal point. By placing transmitters and receivers at ground sites so that the reflection region is over the explosion, we can remotely sense perturbations from distances of hundreds of kilometers. During daylight we have employed radio transmissions in the high frequency (hf) band (3–30 MHz) to monitor explosions. Medium frequencies (mf, .3–3 MHz) are highly absorbed during daylight while very high frequencies (vhf, 30–300 MHz) do not reflect. At night hf transmissions reflect at such high altitudes that detection of weak explosions becomes difficult. Medium frequencies suffer much less attenuation at night and reflect from altitudes that are sensitive to weak explosions.

### 2.1 Nighttime Ionosphere

The electron density distribution in the ionosphere is commonly described in terms of layers although the transition between them is not always distinct. The highest, the *F* layer, usually contains the maximum electron density in the ionosphere attained at altitudes of 200 to 300 km and equal to about  $10^{12} \text{ m}^{-3}$ . The *F* layer persists during the night with only a slightly decreased density although the altitude of the maximum rises. During daylight, the electron density in the lower ionosphere is strongly controlled by solar radiation. At the lowest altitudes, the *D* layer (60–90 km) causes absorption of radio waves propagating to the upper ionosphere; the *D* layer disappears at night. The electron density in the *E* layer (90–120 km) reaches a local maximum of about  $10^{11} \text{ m}^{-3}$  during daylight. Between the *E* and *F* layers there is often a transition layer designated *FI* which disappears at night. In the absence of solar ionizing radiation the phenomenology of the lower ionosphere during nighttime differs markedly from the typical daytime distribution and has been investigated using a variety of techniques: sounding rockets [Smith, 1970], incoherent scatter radar [Shen *et al.*, 1976], and ionograms [Watts, 1957]. On average, there is a maximum in electron density between 100 and 110 km altitude; the value of the maximum depends upon the solar cycle. Wakai [1971] fitted the following line to measurements of peak electron density,  $N_m$ , obtained over a period of three years:  $N_m = 2.21 \times 10^9 (1 + 0.0062R) \text{ m}^{-3}$  where  $R$  is the sunspot number. The source of this peak, which defines what is called the nighttime *E* layer, has been attributed to hydrogen Lyman  $\alpha$  and Lyman  $\beta$  scattered from the geocorona [Ogawa and Tohmatsu, 1966]. Imbedded in this layer, there often are additional layers with much higher density and narrower altitude distributions which are labelled sporadic *E* or  $E_s$ , because of their intermittent existence [Smith, 1970]. The cause of  $E_s$  layers is

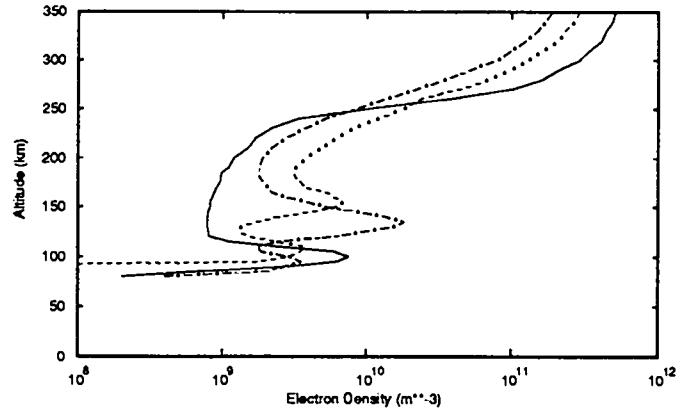


Figure 1: Plots of electron density near local midnight versus altitude for three different dates; two of the nights show intermediate layers in the valley between the *E* layer near 100 km and the *F* layer above 200 km [Wakai, 1971].

generally attributed to concentration of metallic ions of meteoritic origin by gravity waves in the neutral atmosphere [Hermann *et al.*, 1978]. The electron density at altitudes between the top of the nighttime *E* layer at 120 km and the bottom of the *F* layer at 180 km are about 10% of the peak density in the *E* layer under quiet conditions of the geomagnetic field [Wakai, 1971]. However, this valley often displays enhanced electron densities in a form labelled 'intermediate layers.' These layers appear at altitudes of 160 km with a peak concentration that increases with the disturbance level of the magnetic field; their height gradually decreases over a period of hours so that they merge with the nighttime *E* layer. Their origin appears to result from concentration of ionization produced by energetic particles of solar origin [Shen *et al.*, 1976]; the concentration mechanism is attributed to long period waves in the neutral atmosphere (solar tides) inducing ion motion along the magnetic field [Fujitaka and Tohmatsu, 1973]. The peak density can reach levels of one order of magnitude greater than that in the nighttime *E* layer [Wakai, 1971]. Some typical profiles of electron density versus altitude near local midnight are shown in Figure 1; two of the profiles display intermediate layers [Wakai, 1971].

## 2.2 Measurement Technique

If one ignores the effect of the geomagnetic field, the index of refraction of the ionosphere for a radio wave of frequency,  $f$ , is  $\sqrt{1 - f^2/f_N^2}$  where  $f_N$  is called the plasma frequency [Davies, 1990]. The plasma frequency is proportional to the square root of the electron density:  $f_N^2 = Nc^2r_e/\pi$  where  $N$  is the electron density,  $c$  is the speed of light, and  $r_e$  is a constant (the classical electron radius). Using mks units,  $f_N^2 \approx 81N$ . A vertically propagating radio wave will be reflected at the altitude for which its index of refraction is zero; that is, the altitude for which  $f = f_N$ . In Figure 1, the critical frequencies for reflection for the vertical reflection from the *E* layer range from 500 to 800 kHz while they

range from 4 to 6.5 MHz for reflection from the  $F$  layer. For a sunspot number of 100, the critical frequency of this layer is about 540 kHz; thus at night, for distances greater than 600 km, broadcasts in the medium-frequency am band ( $< 1500$  kHz) will reflect from this  $E$  layer [Davies, 1990].

In our technique of remote monitoring of the ionosphere we use oblique propagation rather than vertical; that is, we locate a radio transmitter and receiver at spatially separated sites such that the explosion is close to the mid-path. This geometry makes the reflection process sensitive to acoustic waves propagating directly from the explosion to the ionosphere. It can be shown that oblique propagation at a frequency,  $f$ , is equivalent with some restrictions to vertical propagation at a frequency of  $f \cos \phi_o$  where  $\phi_o$  is the angle of incidence of the ray upon the ionosphere [Davies, 1990]. That is, we can reflect at the same altitude in the ionosphere by increasing the frequency of our obliquely propagating radio transmission as we increase the separation our transmitter and receiver.

We broadcast multiple frequencies from each transmitter location; the frequencies are chosen so that they reflect from sufficiently separated altitudes to allow time delay discrimination of vertically propagating acoustic waves. The use of multiple frequencies also allows some redundancy in the measurements. We detect the high frequency radio signals with Racal 6790GM receivers operated in continuous wave mode which produce a low-passed audio signal at a frequency between 20 to 50 Hz which is digitized and stored. Moreover, we employ a spatial array of antennas at the receive locations so that we could conduct interferometry and array processing of the disturbances.

### 2.3 *Hunters Trophy*

For the Hunters Trophy experiment we employed two transmitter locations, one at Tonopah Test Range (TTR) and the other at the EPA Farm in Area 15 of the NTS; we also employed two receiver locations, one near Well 5e (WL5) in Area 5 of the NTS and the other at Indian Springs AFB (ISP). The map in Figure 2 shows that these locations give sensitive regions over Area 19, Area 12, and Area 3. The primary path for the experiment was TTR-ISP which reflected almost directly over the site of the explosion. The frequencies of the transmissions, 2.83 and 2.93 MHz, were chosen to reflect in the  $E$  layer near 100 km altitude; the frequencies of the two transmit sites were offset by 30 Hz so that they could be recorded simultaneously at each receive site. Figure 2 also shows the disposition of the receive arrays. The explosion was conducted at 1700 UT on Sept. 18, 1992.

The transmissions that we use for monitoring explosions have high phase and amplitude stability; therefore, variations in phase and amplitude of the received signal arise from propagation effects among which the reflection process is the most important. A convenient way of displaying the time variations of the received signal is to plot the power spectrum of the complex amplitude versus time. That is, our received signal can be written as  $a(t) \cos 2\pi ft$  where  $a(t)$  is a complex time series. Our radio receiver and data analysis removes the  $\cos 2\pi ft$  variation which contains no information. Variations in the phase of  $a(t)$  can arise from changes in the length of the propagation path; variations in the magnitude can arise from interference between multiple reflections, from focussing, and

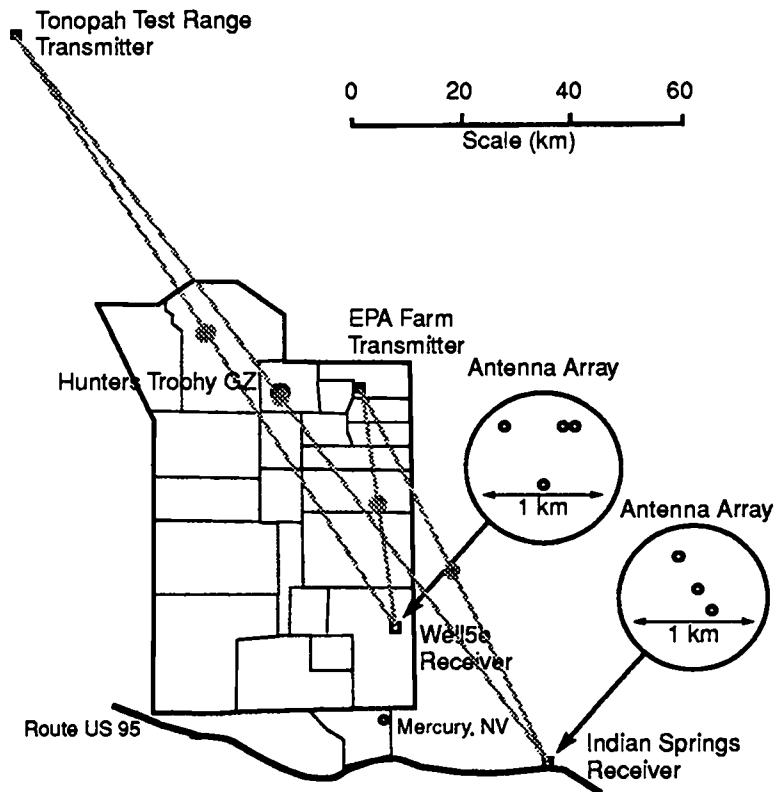


Figure 2: Map of transmit and receive locations for the Hunters Trophy experiment. The path from the Tonopah Test Range to the Indian Springs AFB reflected almost directly over the explosion.

from variations in absorption. The time rate of change  $a(t)$  is relatively slow so that power spectrum will usually show a peak near a frequency of 0 Hz. Figure 3 shows such a plot of the power spectrum versus time between 100 and 600 s after the Hunters Trophy test for the 2.83 MHz transmission between TTR and ISP, that is, the path reflecting almost directly over the explosion. There is a distinct broadening of the spectrum at about 320 s which corresponds to the acoustic travel time to the reflection altitude near 100 km. Such a broadening is also observed on the 2.93 MHz data but with a delay of about 2 s which corresponds to the differential delay to the slightly greater reflection altitude ( $\sim .5$  km) of the higher frequency transmission. The passage of the acoustic wave from the explosion can also cause a frequency or Doppler shift of the received transmission as the phase path of the signal is perturbed; that is, the time rate of change of the phase may be interpreted as a frequency shift. Such a shift may be detected by tracking the centroid of the peak in the power spectrum versus time. Figure 4 plots the frequency of the major peak in the power spectrum between 300 and 350 s after the test for the two frequencies between TTR and ISP. The background fluctuation level is a few hundredths of a Hertz; at about 320 s both frequencies show a negative excursion followed by a positive excursion with a peak-to-peak shift of about 0.14 Hz. The excursion on the higher frequency occurs about 1.9 s after that on the lower; the total duration of the disturbance is about 5 s. There are also changes in the received signal strength accompanying the perturbations as shown in Figure 5. The received power reaches a maximum at about the time of the most negative frequency shift; the combination of the frequency and amplitude changes leads to a broadening of the power spectrum as shown in Figure 3

The perturbation for paths not reflecting directly above SGZ takes a different form as shown in Figure 6 which plots the power spectrum for the 2.93 MHz transmission between TTR and WL5. As shown in Figure 2 the midpath is about 20 km NW of SGZ. The perturbation is spread out in time between 330 and 350 s and appears as peak in frequency that moves from positive to negative Doppler shift. Our interpretation of this effect is that the perturbation produces a scattering from a point at the intersection of the spherically expanding acoustic wave and the horizontal plane of the reflection altitude [Fitzgerald and Carlos, 1992]. The phase path initially decreases as the intersection point approaches midpath producing a positive Doppler shift; after passing through midpath the phase path increases producing a negative Doppler shift.

### 3 Non-Proliferation Experiment

The Non-Proliferation Experiment (NPE) was designed to compare measurements that have been obtained with various diagnostics that have been used to characterize nuclear explosions with the same measurements using a large chemical explosion as a source. A charge of 1.29 kt of a mixture of ammonium nitrate and fuel oil (ANFO) was detonated in a cavity in Area 12 of NTS near the site of the Hunters Trophy experiment at 7:01 UT on Sept. 22, 1993 [Zucca, 1993].

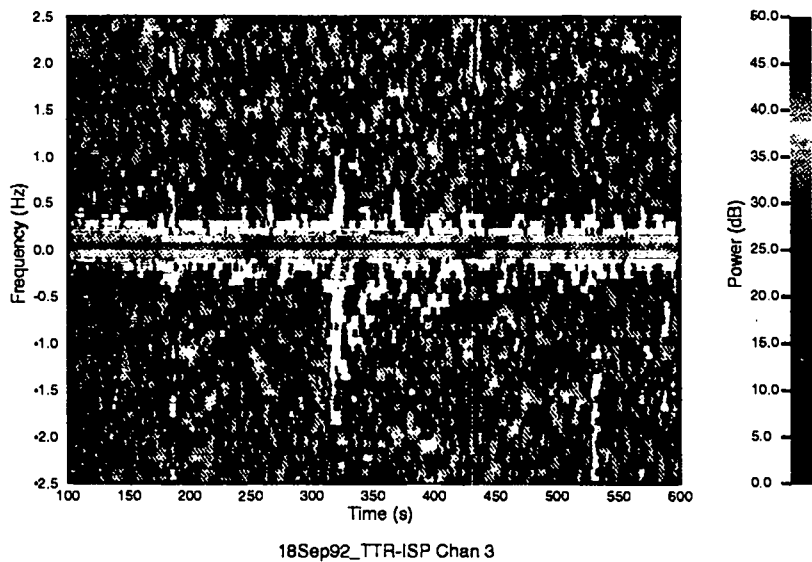


Figure 3: Power spectra versus time for the 2.83 MHz transmission from the Tonopah Test Range received at Indian Springs during the period from 100 to 600 s after the Hunters Trophy test. There is a broadening of the spectrum at about 320 s corresponding to the passage of the acoustic wave through the reflection altitude.

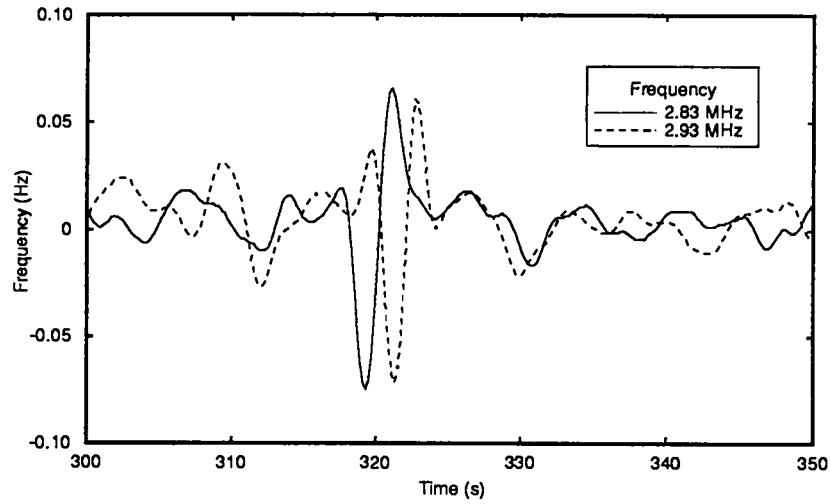


Figure 4: Frequency of the centroid of the 2.83 and 2.93 MHz transmissions from Tonopah Test Range received at Indian Springs during the period from 300 to 350 s after the Hunters Trophy test. The perturbations at about 320 s result from the passage of the acoustic wave through the slightly different reflection altitudes of the two frequencies.

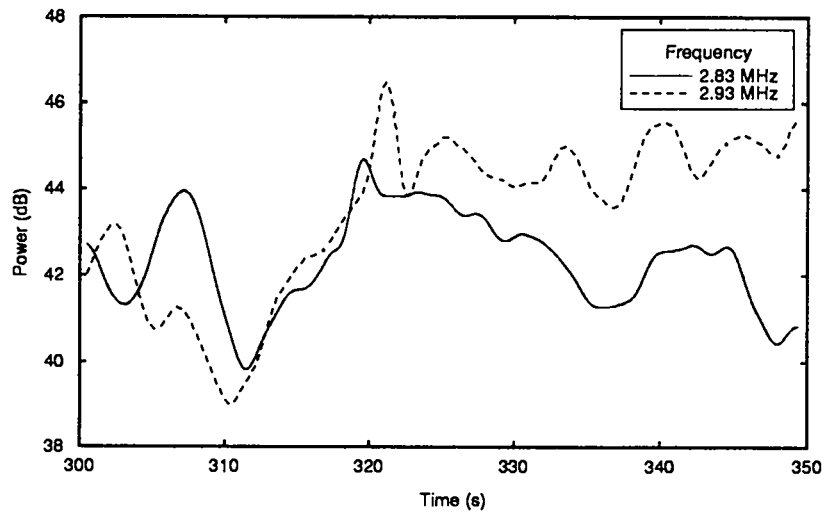


Figure 5: Power of the 2.83 and 2.93 MHz transmissions from Tonopah Test Range received at Indian Springs during the period from 300 to 350 s after the Hunters Trophy test. The perturbations reach a maximum power about the time of the most negative frequency shift.

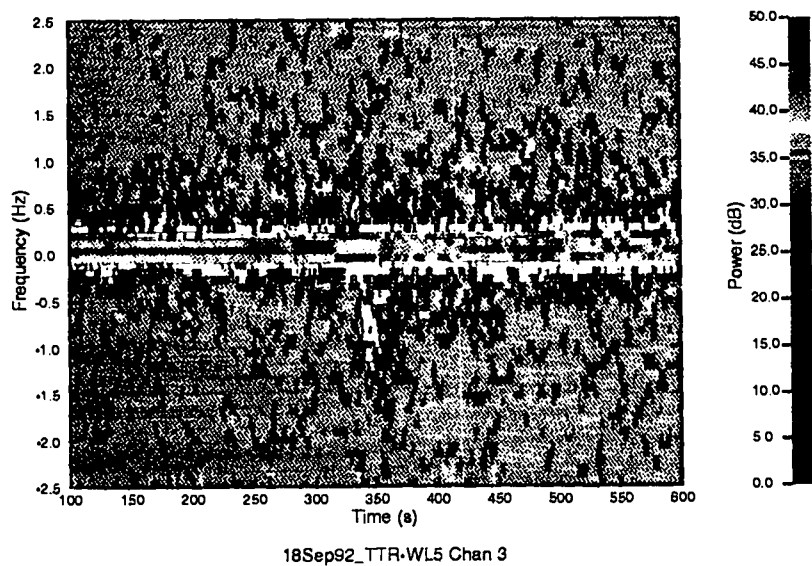


Figure 6: Power spectra versus time for the 2.93 MHz transmission from the Tonopah Test Range received at Well 5e during the period from 100 to 600 s after the Hunters Trophy test. There is a perturbation between 330 and 350 s during which a low amplitude peak moves from positive to negative frequency shift.

### 3.1 Experiment

Because the NPE was scheduled for the middle of the night, the network that we deployed for the Hunters Trophy event (Figure 2) would have had to use frequencies of less than 1 MHz to reflect in the *E* layer. We are uncertain of how well our transmitters would perform at such a low frequency; moreover, we did not have frequency authorization to operate in the am broadcast band. Therefore we chose instead to monitor the carrier of am broadcast stations near Las Vegas from a site near Tonopah, NV; the midpath for this geometry is over Area 12 of NTS. The frequencies of the monitored broadcasts were 720 (KDWN), 840 (KVEG), 920 (KORK), and 1140 kHz (KLUC); the signals at 720 and 840 kHz could be identified and were primarily from Las Vegas. At the two higher frequencies many stations were transmitting and the interference prevented any identification of the Las Vegas broadcasts. The stations at 720 and 840 kHz use powerful transmissions of 50 and 25 kW respectively and have only a limited competition from other broadcasts; the stations at 920 and 1140 kHz are limited to low power operation [Sennitt, 1993]. Figure 7 shows the locations of the transmit and receive sites in relation to the NPE explosion. The receiver site was located at 38.07° N, 117.12° W; the KDWN transmitter is located in Henderson, NV (36.04° N, 114.98° W) while the KVEG transmitter is located outside of Las Vegas at 36.43° N, 115.28° W. The location of the NPE event was 37.20° N, 116.21° W so that the mid-path of the KDWN transmission was 23 km from surface ground zero (SGZ) while the mid-path of the KVEG transmissions was 5 km from SGZ [Zucca, 1993]. We deployed two receive antennas separated by 460 m in the North-South direction; we monitored the four transmissions with each of the receive antennas using Racal 6790GM receivers operated in continuous wave mode with a narrow bandwidth filter that eliminated the sidebands caused by the amplitude modulation. Data storage and reduction were the same as described above for the Hunters Trophy experiment.

### 3.2 Tonopah Results

Figure 8 shows the power spectra versus time for the 720 kHz frequency received at Tonopah for the period of 100 to 600 s after the NPE explosion; we identify the peak near 2.5 Hz as the carrier of the Las Vegas broadcast because it was the major peak in this data. The offset of 2.5 Hz is mostly a result of the difference in the reference oscillator at the transmitter compared to the Rubidium oscillator reference of our receivers and does not represent an ionospheric reflection effect. There is a weaker carrier at about 1 Hz which has not been identified. The 2.5 Hz peak displays long and short term fading indicative of ionospheric propagation effects. This power spectral display indicates that there were no short duration perturbations in the this time interval of likely effects which could be attributed to the explosion at the 60 dB signal-to-noise level. Figure 9 is a similar display of power spectra versus time for the 840 kHz frequency received at Tonopah. The peak near 1 Hz is attributed to the Las Vegas broadcast; there is a weaker peak near 3 Hz that has not been identified. Again the offset of the 1 Hz peak is caused by a difference in the reference oscillator; there is also a long period drift of the centroid of the peak which is caused by an unstable reference at the transmitter. The peak does show short period fading indicative of interference of two

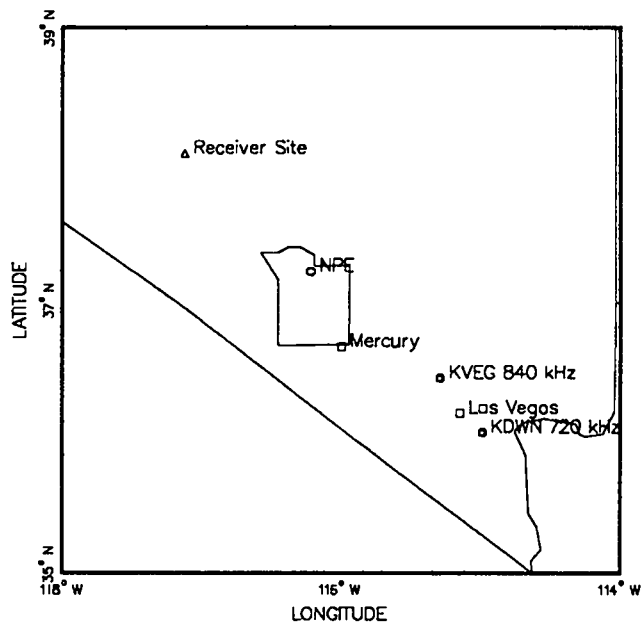


Figure 7: Map of transmit and receive locations for the Nonproliferation Experiment (NPE). A receiver site near Tonopah, NV, was used to monitor broadcast stations near Las Vegas.

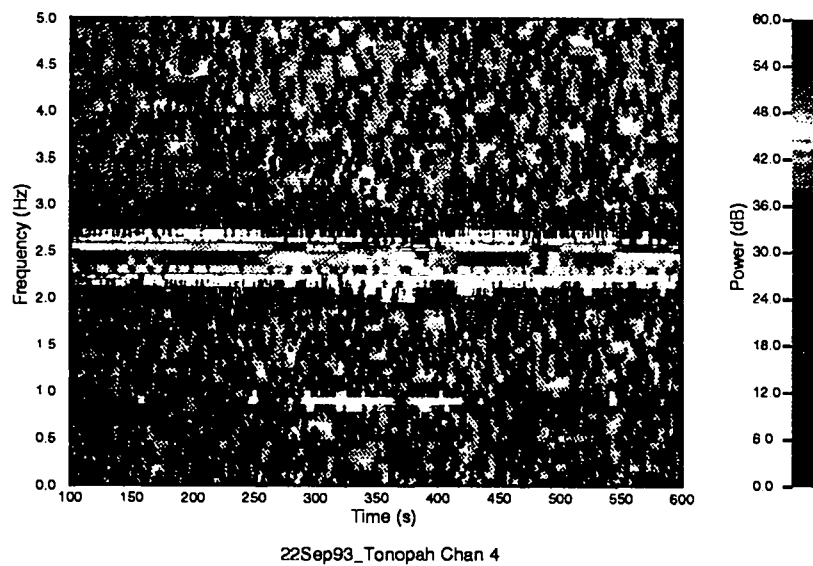


Figure 8: Power spectra versus time for the 720 kHz transmission received at Tonopah during the period from 100 to 600 s after the NPE explosion. The peak near 2.5 Hz is the carrier of the Las Vegas broadcast; no perturbations attributable to explosion effects are evident.

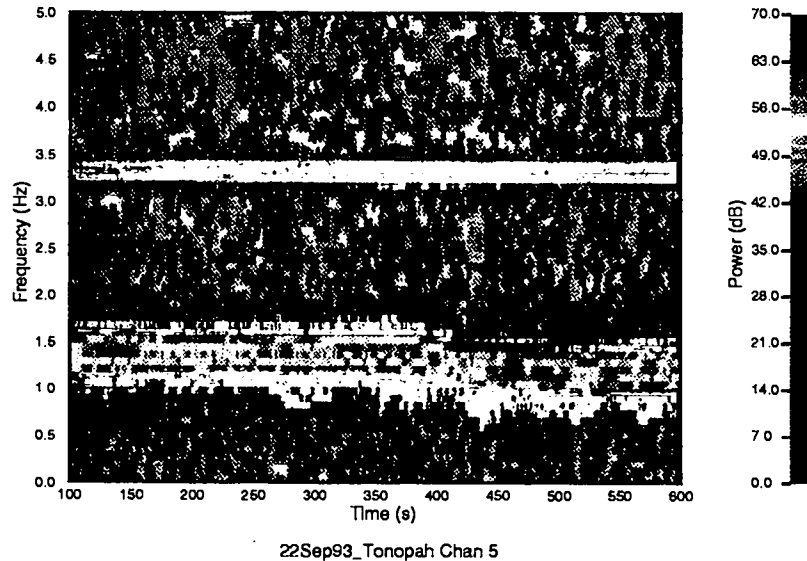


Figure 9: Power spectra versus time for the 840 kHz transmission received at Tonopah during the period from 100 to 600 s after the NPE explosion. The peak near 1 Hz is the carrier of the Las Vegas broadcast; no perturbations attributable to explosion effects are evident.

or more propagation modes. There is no short duration perturbations during this time period which could be attributed to effects of the NPE explosion at the 70 dB signal-to-noise ratio.

The passage of the acoustic wave from the explosion can also cause a frequency or Doppler shift of the received transmission as the phase path of the signal is perturbed. Such a shift may be detected by tracking the centroid of the peak in the power spectrum versus time. Figure 10 shows the frequency of the peak of the 720 kHz transmission between 100 and 600 s after the NPE explosion. Fluctuations range from a few hundredths to a few tenths of a Hertz; the large fluctuations are probably the result of mode interference or difficulty in locating the peak when the signal amplitude drops. No effect of the explosion is apparent above this fluctuation level. Figure 11 shows a similar plot for the 840 kHz transmission; the fluctuation in this data is greater than that in the 720 kHz data and results from the presence of two or more modes closely spaced in frequency which beat against each other and cause the apparent frequency of the peak to fluctuate. Again no perturbation attributable to the NPE explosion is present above these fluctuations. We can compare the frequency of the peak for the two different antennas for the 720 kHz frequency. Figure 12 plots the frequency of the peak for the period between 200 and 300 s after the NPE explosion for the

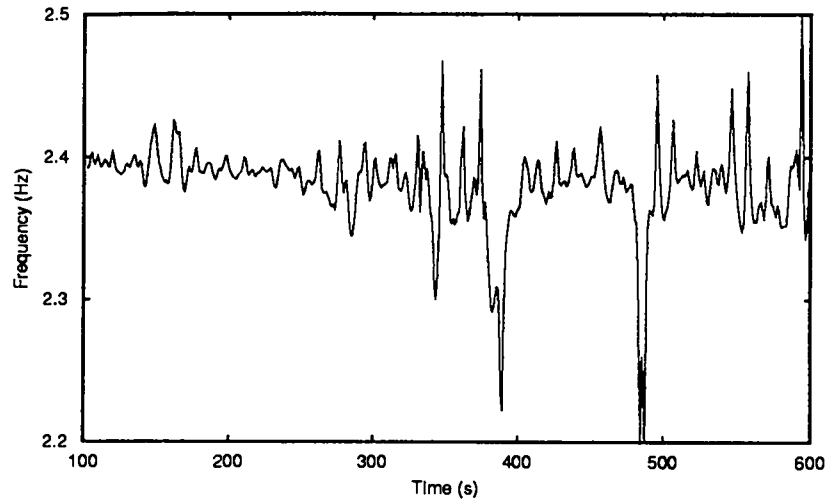


Figure 10: Frequency of the centroid of the 720 kHz transmission received at Tonopah during the period from 100 to 600 s after the NPE explosion. No perturbations attributable to explosion effects are evident above the background fluctuation level.

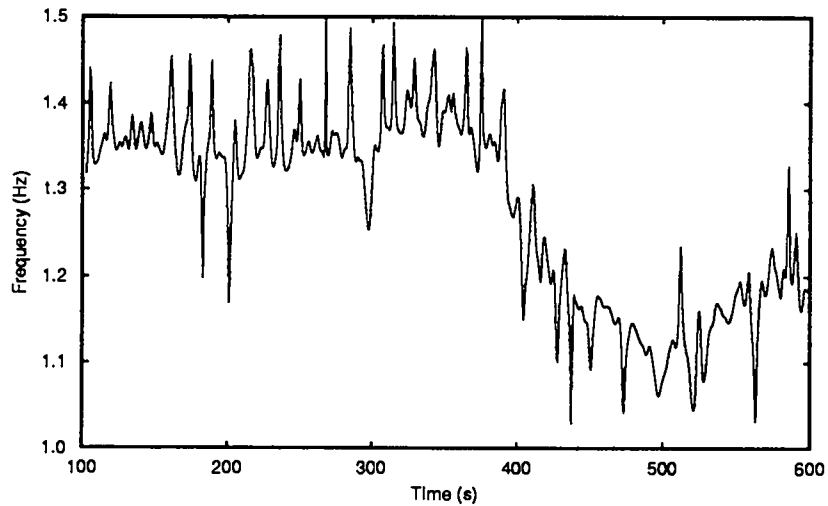


Figure 11: Frequency of the centroid of the 840 kHz transmission received at Tonopah during the period from 100 to 600 s after the NPE explosion. No perturbations attributable to explosion effects are evident above the background fluctuation level.

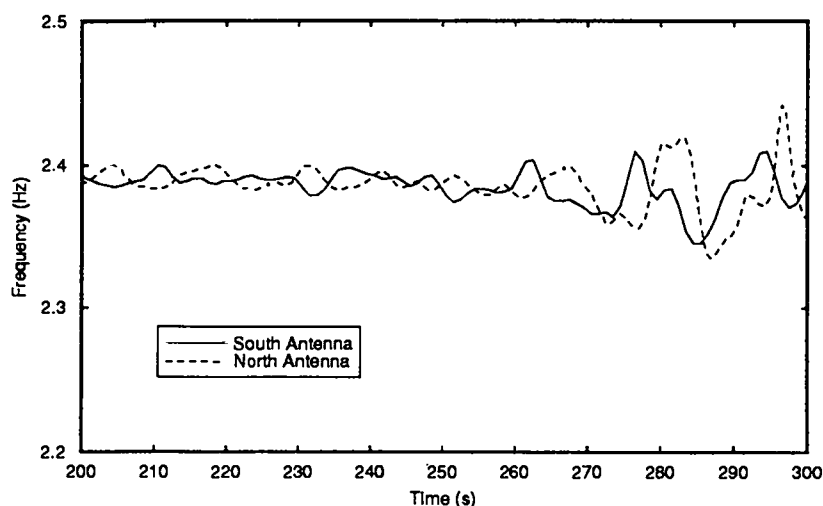


Figure 12: Comparison of the frequency of the centroid of the 720 kHz transmission received at the two antennas at Tonopah during the period from 200 to 300 s after the NPE explosion. The fluctuations appear correlated but with a time delay of about 5 s between them. The antennas were separated by 460 m in the North–South direction.

two different antennas. The plot indicates that the fluctuations are correlated but with a time delay of about 5 s between the two antennas. This indicates that they are of ionospheric origin and are not fluctuations in the frequency of the transmitter. Such fluctuations are likely to be caused by variations in electron density induced by naturally occurring acoustic gravity waves in the neutral atmosphere.

### 3.3 *Los Alamos Results*

As a check on the stability of the broadcast transmissions we monitored the 720 and 840 kHz frequencies using receivers at Los Alamos; we did not expect to see any effects of the NPE explosion in this data because the reflection point would be too far away. Figure 13 shows the frequency of the peak of the 720 kHz transmission received at Los Alamos in the same format as Figure 10. Comparison of the two figures indicates that fluctuations in the transmissions frequency were less than a few hundredths of a Hertz during this time period; there were larger fluctuations at other time periods. Similarly Figure 14 shows the frequency of the peak of the 840 kHz transmission received at Los Alamos; comparison with Figure 11 indicates that the long period trends were caused by drift in the transmitter frequency. Such drifts were observed throughout the night.

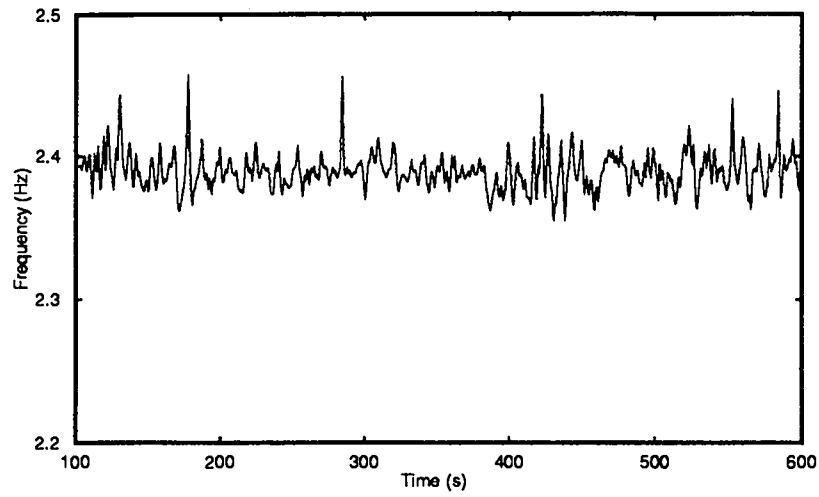


Figure 13: Frequency of the centroid of the 720 kHz transmission received at Los Alamos during the period from 100 to 600 s after the NPE explosion. Comparison to the Tonopah results indicates that the transmitter frequency was stable to less than a few hundredths of Hertz during this time period.

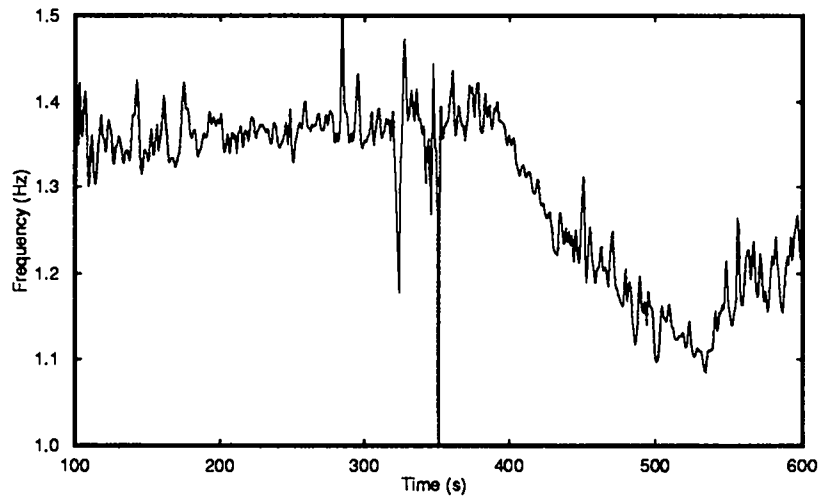


Figure 14: Frequency of the centroid of the 840 kHz transmission received at Los Alamos during the period from 100 to 600 s after the NPE explosion. Comparison to the Tonopah results shows common long period drifts caused by drift of the transmitter frequency.

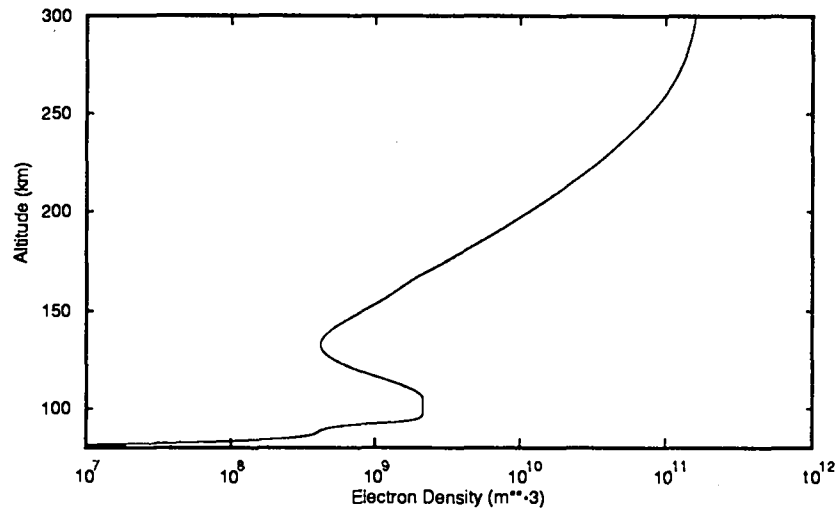


Figure 15: Model electron density versus altitude obtained from the International Reference Ionosphere for a sunspot number,  $R = 40$ , and a local time of 2300 [Rawer and Bradley, 1987].

## 4 Discussion

Preliminary results indicate that the ground motion near SGZ for the NPE was similar to that for Hunters Trophy [Taylor, 1993]. It is likely that an acoustic pulse of similar amplitude and duration was produced for the two events; indeed, infrasound from the NPE was detected at St. George, Utah [Whitaker, 1993]. The absence of a definite signature in our data following the NPE is therefore puzzling.

### 4.1 Propagation

One possible explanation for our negative results is that we did not achieve reflection from the  $E$  Layer that we desired because the electron density was low. Solar activity as measured by the sunspot number,  $R$ , had decreased to a very low level of 40 during the week preceding the NPE. As indicated above, the peak electron density in the nighttime  $E$  Layer decreases with decreasing values of  $R$  and could have reached a level that would not have supported  $E$  Layer propagation between the 720 kHz broadcast transmitter and our receiver station. To test this hypothesis, we have computed a numerical raytrace for the 720 kHz frequency using a model ionosphere. The electron density distribution versus altitude was obtained from the International Reference Ionosphere (IRI) computer model using a sunspot number,  $R = 40$ , and a local time of 2300 [Rawer and Bradley, 1987]. A plot of the model density is shown in Figure 15; the maximum density in the  $E$  Layer is  $2.14 \times 10^9 \text{ m}^{-3}$ . Figure 16 shows the results of the raytrace for a frequency of 720 kHz (ordinary magneto-ionic mode);  $T$  represents the location of the transmitter and  $R$  the location of the receiver. The

different lines show raypaths with different elevation angles; the highest elevation angle path represents a homed ray connecting the transmitter and receiver. This ray reflects in the  $F$  layer at an altitude of about 180 km. The low angle rays which reflect in the  $E$  layer approach to within about 40 km of the receiver but then penetrate the  $E$  layer and return to the ground at much greater distances. The other frequencies monitored were higher than 720 kHz and would penetrate the  $E$  layer at even lower elevation angles and thus would not approach as close to the receiver location. The extraordinary magneto-ionic mode has lower critical frequency than the ordinary mode and would also penetrate the  $E$  layer at lower elevation angles. These results indicate that the likely propagation for the frequencies monitored during the NPE experiment was via reflection in the  $F$  layer at altitudes above 150 km. Because the monitoring technique that we employed detects only the continuous wave carrier we do not have any information on the reflection altitude of the transmissions to confirm these raytraces. There should have been at least two propagation paths via the two magneto-ionic modes in either case which is the likely cause of the observed multi-path. Since the acoustic wave from the explosion would be greatly dissipated at the predicted reflection altitudes, we would expect that the ionospheric signature to be below the level of natural propagation fluctuations and not detectable.

#### 4.2 Prediction of Effects

We may predict the level of effects that would have been observed if the 720 kHz transmission had reflected in the  $E$  layer for comparison to the data obtained during the NPE experiment. The first step is to obtain a description of the expected acoustic wave; we do this by assuming that the wave was comparable to that produced by the Hunters Trophy test. A description of the latter may be derived by matching numerical simulations of the frequency shift versus time to the data (Figure 4). We assume that the waveform has a simple symmetric profile consisting of a leading overdensity followed by an underdensity; the leading and trailing edges of the waveform are steep while there is a linear change in density in between. This waveform is called an N-wave because its profile has an N shape; the perturbation,  $d(z)$ , may be written

$$d(z) = \frac{az}{l} \left[ \tanh \frac{z + l/2}{w} - \tanh \frac{z - l/2}{w} \right] \quad (1)$$

where  $z$  is distance relative to the center of the perturbation,  $a$  is the amplitude,  $l$  is the size of the perturbation, and  $w$  is the size of the leading and trailing edges. We assume that the acoustic perturbation radiates outward from SGZ at the sound speed,  $c$ , of 300 m/s without deformation; the local electron density,  $n_e(\mathbf{r})$ , at point  $\mathbf{r} = (x, y, z)$  is altered by the factor,  $d(r - ct)$ . We use a model ionosphere for  $n_e$  derived from IRI for the conditions holding during the Hunters Trophy test. We then raytrace numerically to an accuracy of <1 m every 0.1 s as the perturbation advances through the reflection altitude which for the 2.83 MHz transmission was at 94 km altitude. The raytrace calculates the phase path at each time from which we can derive a synthetic complex time series similar to the actual data. We then can analyse the synthetic time series to find the centroid of the peak frequency in the



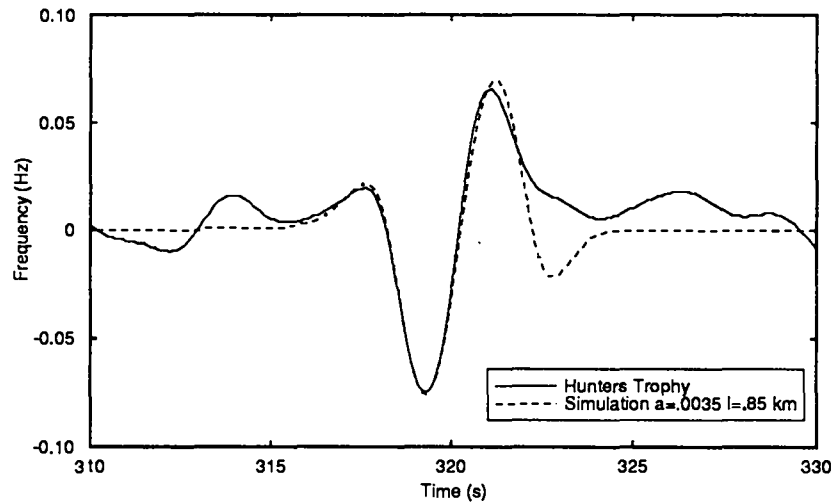


Figure 17: Comparison of the measured Doppler shift for Hunters Trophy and that predicted for acoustic wave with an amplitude of 0.35% and a length of 0.85 km.

same manner as for the data as shown in Figure 4. The results of such a simulation using inputs of  $a = .0035$ ,  $l = 0.85$  km and  $w = .1$  km (Figure 17) produce a good match to the measured perturbation for Hunters Trophy which is also plotted.

With the parameters derived from the Hunters Trophy simulation we can simulate effects that would be observed at nighttime using a 720 kHz frequency. We take the path used during the NPE experiment but place the explosion at the midpoint rather than 20 km distant; we also use an ionosphere computed for a sunspot number of 100 rather than 40. Then the 720 kHz frequency reflects in the  $E$  layer at an altitude of about 94 km. We then raytrace every 0.1 s to obtain a complex time series in the same manner as for the Hunters Trophy simulation; the results are shown in Figure 18. The predicted frequency perturbation is smaller than that for the 2.83 MHz, daytime simulation; part of the difference is due to the difference in frequencies since, for the same phase path change in meters, the change in cycles, which is inversely proportional to the wavelength, would be smaller at the lower frequency. Comparison to the measured frequency shifts shown in Figures 10 and 11 indicate that the predicted perturbation is less than the fluctuations in the data while the the Hunters Trophy perturbation is greater than the fluctuations. We would expect that the natural fluctuations would also be roughly proportional to frequency and so their level would be lower at 720 kHz than at 2.83 MHz. This discrepancy is consistent with a reflection of the 720 kHz at a higher altitude than the  $E$  layer because the amplitude of the acoustic-gravity waves causing the natural propagation fluctuations increases with altitude so that the  $F$  layer is usually more disturbed than the  $E$ . Another contribution to the discrepancy is the definite presence of multiple modes with slightly different Doppler shifts during the nighttime; because they fade at different times they can produce increased

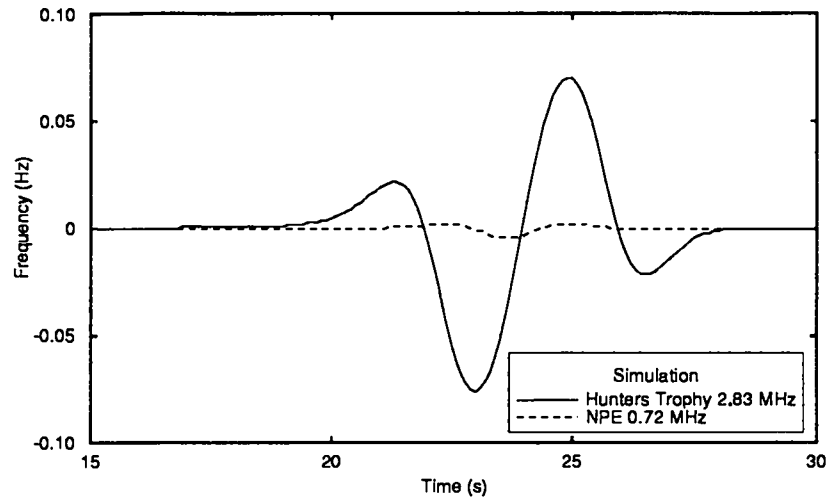


Figure 18: Comparison of the measured Doppler shift for Hunters Trophy and that predicted for acoustic wave with an amplitude of 0.35% for the Hunters Trophy conditions and the predicted Doppler shift for the same acoustic wave for the NPE conditions altered to achieve *E* layer reflection.

noise in the frequency estimate. It is likely that these multiple reflections are ordinary (*o*) and extraordinary (*x*) modes; during the daytime the *x* mode is more highly absorbed than the *o* mode so that essentially the *E* layer produces only one reflection path. From our simulation we can also predict the behavior of the power spectrum of the received signal versus time for comparison to the experimental results shown in Figures 8 and 9. Figure 19 shows the expected perturbation as a broadening of the power spectrum at the -30 dB level relative to the peak; although weak, this perturbation would be detectable under the conditions of the NPE experiment.

### 4.3 Mining Explosions

In a previous report we discussed the ionospheric detection of acoustic waves produced by mining explosions [Fitzgerald, 1993]; these mining explosions were conducted during the daytime and our measurement system employed reflection of high frequency transmissions in an arrangement similar to that discussed above for the Hunters Trophy explosion. Figure 20 plots the centroid of the frequency for one of the transmissions following what was categorized as a large mining explosion ( $m_L = 2.9$ ). We ascribe the perturbation in frequency centered at 298 s and persisting for about 5 s to the airblast generated by the explosion. This perturbation may be compared to the results for the Hunters Trophy shown in Figure 4. The form of the perturbation is similar for the two sources indicating that acoustic propagation effects have removed any difference caused by the initial conditions. The strength of the perturbation in frequency shift and the time durations are smaller for

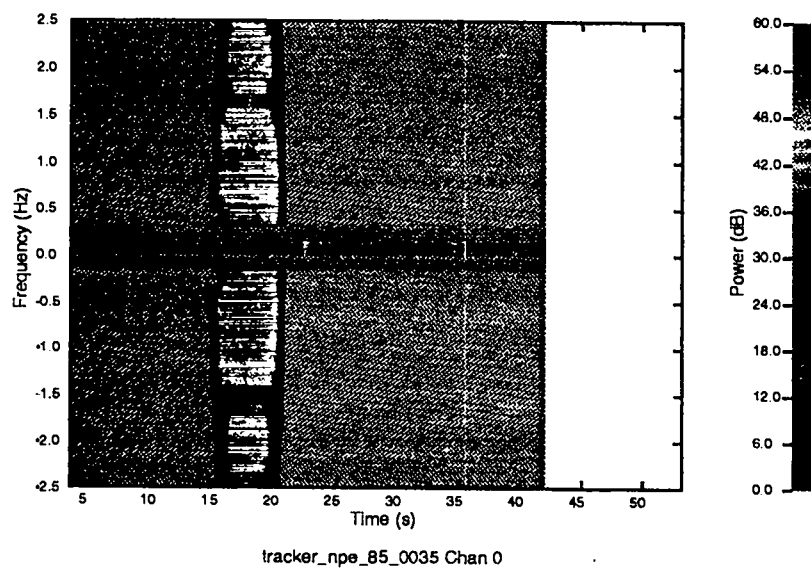


Figure 19: Predicted behavior of the power spectrum for the NPE simulation altered to achieve *E* layer reflection. The broadening of the spectrum would have been detectable under the NPE experimental conditions.

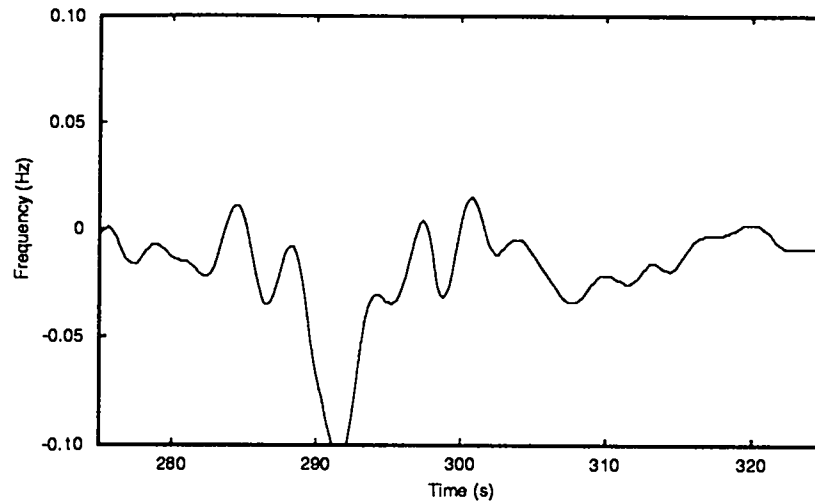


Figure 20: Frequency of the centroid of a 4.15 MHz transmission versus time after a large mining explosion [Fitzgerald, 1993]. We attribute the perturbation centered at 298 s to the passage of the acoustic wave from the explosion through the reflection altitude.

the mining explosion. There was a significant difference in seismic magnitude for the two events; Hunters Trophy had a body wave magnitude,  $m_b$ , of 4.2, versus the mining explosion which had  $m_b \lesssim 3.2$  [Wallace, 1993]. The difference in seismic magnitudes for similar acoustic amplitudes could serve as a discriminant to distinguish the two types of sources [Fitzgerald, 1993].

Given that the acoustic perturbation from a large mining explosion will be of similar amplitude and duration to that expected for the NPE, nighttime mining explosions will also be difficult to detect. On the other hand, most mining explosions are detonated during the daytime. Riviere-Barbier [1992] reported the hourly distribution of 443 seismic events in six sub-areas of the Kola Peninsula of Russia; most of the events were mining explosions. In all except one of the sub-areas the mining explosions occurred almost exclusively during the day; in fact the explosions tended to be clustered either a few hours before noon or a few hours after noon. Although mining practice varies between countries and even within countries, it is likely that most of the events that will need to be discriminated will occur during daylight and that our ionospheric systems will be useful. So far, no nighttime mining explosions have occurred during our monitoring periods; we will, of course, try to obtain such nighttime data in future monitoring activity of mining or other explosions.

## 5 Conclusion

The detection of explosions during nighttime using ionospheric techniques remains problematical. Previous measurements of underground explosions indicate that using radio

reflection of transmissions in the high frequency band is not effective because the sensitive altitude is so high that the acoustic waves from the explosion have dissipated. Our recent measurements in conjunction with the Non-Proliferation Experiment show that it is possible to use broadcast stations in the medium-frequency band as radio beacons to monitor the ionosphere above an explosion during the nighttime. Our results indicate that there were no effects that we could attribute to acoustic waves from the explosion although our model calculations indicate that an observable perturbation should have occurred if the desired propagation had been achieved. It is likely that because of an exceptionally low electron density the monitored transmissions reflected at altitudes too high to be useful. Although discouraging, this is only the first attempt using a new technique and deserves to be repeated with another source. It does indicate that it will be difficult to use ionospheric techniques to monitor explosions during the nighttime. However, the goal of the current project is to develop techniques to discriminate sources such as mining explosions which occur primarily during the daytime.

## 6 Acknowledgement

This work was performed under the auspices of the U. S. Department of Energy by Los Alamos National Laboratory under contract W-7405-ENG-36. Alfred Fernandez, Anthony Rose, and William Spurgeon of Los Alamos participated in the fielding and data collection for the Non-Proliferation experiment. Robert Carlos and Harold DeHaven of Los Alamos participated in the fielding and data collection for the Hunters Trophy experiment. Ray traces and the Doppler shift calculation presented in this report were obtained using the TRACKER computer code developed by Paul Argo of Los Alamos.

## 7 References

Davies, Kenneth, *Ionospheric Radio*, Peter Peregrinus, 1990.

Fitzgerald, T. J., Detection of mining explosions using ionospheric techniques, *Rept. LAUR-93-3557*, Los Alamos National Laboratory, Los Alamos, NM, October, 1993.

Fitzgerald, T. J., and R. C. Carlos, The effects of 450 kg surface explosions at the E layer of the ionosphere, *Rept. LAUR-92-3393*, Los Alamos National Laboratory, Los Alamos, NM, October, 1992.

Fujitaka, K., and T. Tohmatsu, A tidal theory of the ionospheric intermediate level, *J. Atmos. Terr. Phys.*, 35, 425-438, 1973.

Hermann, U., P. Eberhardt, M. A. Hidalgo, E. Kopp, and L. G. Smith, Metal ions and isotopes in sporadic E-layers during the Perseid meteor shower, *Space Res.*, 18, 249, 1978.

Ogawa, T. and T. Tohmatsu, Photoelectronic processes in the upper atmosphere, 2, The hydrogen and helium ultraviolet glow as an origin of the nighttime ionosphere, *Rep. Ionos. Space. Res. Japan*, 20, 1966.

Rawer, K. and P. A. Bradley, eds., International Reference Ionosphere—Status 1986/87, *Advances in Space Research*, 7, (6)1–129, 1987.

Riviere-Barbier, F., Identification of Kola peninsula events, *Rept. C92-04*, Science Applications International Corporation, Center for Seismic Studies, Arlington, VA, November, 1992.

Sennitt, A. G., ed., *World Radio TV Handbook*, Billboard Books, 1993.

Shen, J. S., W. E. Swartz, D. T. Farley, and R. M. Harper, Ionization layers in the nighttime *E* region valley above Arecibo, *J. Geophys. Res.*, 31, 5517-5526, 1976.

Smith, L. G., A sequence of rocket observations of night-time sporadic-E, *J. Atmos. Terr. Phys.*, 32, 1247–1257, 1970.

Taylor, S., Los Alamos National Laboratory, Personal communication, 1993.

Watts, J. M., Complete night of vertical-incidence ionosphere soundings covering frequency range from 50 kc/s to 25 Mc/s, *J. Geophys. Res.*, 62, 484-485, 1957.

Wakai, N., Study on the nighttime *E* region and its effects on the radio wave propagation, *J. Radio Research Laboratories*, 18, 245–348, 1971.

Wallace, T., University of Arizona, Personal communication, 1993.

Whitaker, R., Los Alamos National Laboratory, Personal communication, 1993.

Zucca, J., DOE Non-Proliferation Experiment includes seismic data, *EOS, Trans. AGU*, 74, 587, 1993.

LOS ALAMOS NAT'L LAB.  
IS-4 REPORT SECTION  
RECEIVED

94 FEB 18 AM 7 52